Magnetic birefringence and the domain structure of antiferromagnetic cobalt carbonate

N. F. Kharchenko, V. V. Eremenko, and O. P. Tutakina
Physico-technical Institute of Low Temperatures, Ukrainian Academy of Sciences
(Submitted July 7, 1972)
Zh. Eksp. Teor. Fiz. **64**, 1326-1335 (April 1973)

The transformation of an optically uniaxial cobalt carbonate crystal into a biaxial one during antiferromagnetic ordering is observed by the conoscope technique. At 4.2°K, the angle between the optical axes is 3.2° and the birefringence perpendicular to the basal plane is 2.5×10^{-4} for the sodium D line. The principal axes n_m and n_g of the optical indicatrix are respectively parallel and perpendicular to the weak ferromagnetic moment vector. Magnetic domains are observed visually in a magnetic field below the saturation field strength. The domain structure of cobalt carbonate in a magnetic field may be visualized as consisting of plane layers parallel to the basal plane, these layers in turn being divided into parallel strips by transverse interfaces. With increase of field strength the width of the domain bands with the transverse boundaries increases and the number of the bands increases. The boundaries in this case tend to become perpendicular to the magnetic field vector and parallel to the symmetry planes.

1. INTRODUCTION

A unique case of antiferromagnetic domain structure is found in the domain structure of antiferromagnets with weak ferromagnetism, in which the domains can be the result of demagnetizing fields that are due to the existence of a weak ferromagnetic moment[1]. In the thoroughly investigated rhombohedral antiferromagnets, which are characterized by negative magnetic anisotropy, the ferromagnetic moment lies in the basal plane. This circumstance makes it difficult to investigate their domain structures by means of a simple and convenient method that makes use of the analog of the Faraday effect in magnetically ordered crystals, and makes it possible to study the domain structure in the interior of the sample. This method requires an experimental geometry in which the light propagates at large angles to the optical axis. But then the magnetic rotation of the plane of polarization is strongly masked by the natural linear birefringence. On the other hand, another magnetooptical effect can turn out to be quite effective, namely magnetic linear birefringence, which frequently reaches 10^{-4} in magnetodielectrics[2]. To assess the possibility of using magnetic birefringence for the observation of domains in rhombohedral antiferromagnetics with weak ferromagnetism, we have investigated the antiferromagnetic cobalt carbonate, which is transparent in the visible region of the spectrum.

2. SAMPLES AND PROCEDURE

The cobalt carbonate crystal belong to class D_{3d} of the trigonal syngony. It has two magnetic ions per unit cell. It goes over into an antiferromagnetic state with weak ferromagnetism below the magnetic-ordering temperature $T_N = 18°K$[3]. The spontaneous ferromagnetic moment, with a value on the order of 46 cgs emu/cm^3, lies in the basal plane, and the direction of easy magnetization coincides with the twofold crystallographic axes. The energy of the hexagonal anisotropy in the basal plane is equal to 656 erg-cm^{-3}, and the energy of the critical field in the direction of the difficult magnetization is 260 Oe at 4.2°K[3,4]. According to neutron-diffraction investigations[5], the magnetic moments of the sublattices are inclined at a small angle to the vertical symmetry plane and do not lie in the basal plane, but make an angle close to 46° with the trigonal axis.

From the optical point of view, cobalt carbonate above T_N is a negative uniaxial crystal. The principal refractive indices at room temperature for the 5890 Å D line of sodium are $n_o = 1.855$ and $n_e = 1.600$[6]. The visible absorption spectrum of $CoCO_3$ contains several broad bands that become much narrower when it is cooled to low temperatures, and the absorption coefficient in the transparency region does not exceed several cm^{-1}[7]. The investigated samples took the form of plane-parallel and wedge-like plates with approximate dimensions $2 \times 1 \times 0.5$ nm. The plates were cut from artificial single-crystal cobalt carbonate grown by the hydrothermal method at the Crystallography Institute of the USSR Academy of Sciences. The sample was oriented in the plane parallel to the basal plane of the crystal with the aid of an x-ray diffraction analysis and visual observation of the natural cleaved surfaces of the crystal. The adjustment error did not exceed 2°. The sample was either immersed in liquid helium, or was placed into a copper capsule, with the aid of liners that ensured free fastening, and the capsule was then securely mounted on a copper cold finger. The sample temperature was measured with a copper-constantan thermocouple glued to the sample, and could range from temperatures above T_N down to 10°K. A magnetic field of intensity up to 7 kOe was applied parallel to the basal plane. The accuracy with which the optical axis was set perpendicular to the magnetic field was monitored by observing the conoscopic figures. The construction of the sample holder made it possible to rotate the sample placed in helium about an axis perpendicular to the external field.

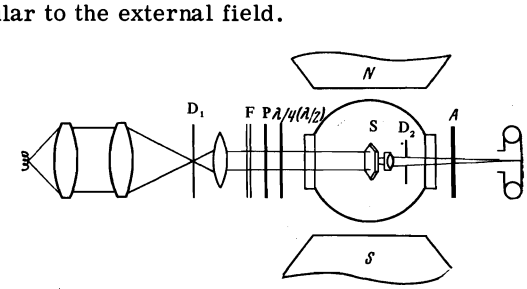

FIG. 1. Optical system of the setup for domain observation

The magnetic birefringence was investigated at different sample temperatures in the direction of the trigonal axis of the crystal by the method of conoscopic figures. We measured the acute angle 2V between the optical axes of the cobalt carbonate magnetized to saturation and then, knowing the refractive indices for the ordinary and extraordinary rays in the magnetic crystal, we estimated the magnetic birefringence in the direction of the angle bisector.

The optical system of the setup for the study of the domain structure is shown in Fig. 1. A distinguishing feature of the system is the small aperture angle of the incident light beam, which should be smaller than the angle between the optical axes. In the experiment, the aperture angle was no more than 1.5°. In addition, to decrease the amount of scattered light, the beam was limited with a diaphragm also after passing through the sample. Visual observation of the domain structure was carried out with the aid of a microscope introduced inside the cryostat. The sample was placed between crossed polarizers. To increase the contrast and to determine the axes of the indicatrix in individual domains, we used chromatic 90° and 180° linear phase plates made of mica. The light source was an incandescent lamp.

3. MAGNETIC BIREFRINGENCE

In the case of magnetic ordering, the trigonal symmetry of cobalt carbonate was lowered, and, depending on the orientation of the magnetic sublattices, its optical properties become the same as the properties of crystals of monoclinic or triclinic syngony. The direction of the optical axes and the magnitude of the magnetic birefringence could be determined by examining the deformation of the optical indicatrix of the crystal on going to the antiferromagnetic state.

Neglecting the gyrotropic effects, the indicatrix equation can be written in the form[8,9]

$$B_{ij}x_ix_j = 1, \tag{1}$$

where $B_{ij} = \epsilon_{ij}^{-1} = B_{ij}^0 + \Delta B_{ij}$. Confining ourselves to effects quadratic in the magnetic moment, we can write[10]

$$\Delta B_{ij} = \alpha_{ijkl}m_km_l + \beta_{ijkl}l_kl_l + c_{ijkl}m_kl_l. \tag{2}$$

Henceforth, owing to the small values of the spontaneous magnetic moment m, we neglect the contributions connected with this moment. The polar fourth-rank i-tensor β_{ijkl} in (2), which is symmetrical in the index pairs, describes both the primary effect of magnetic birefringence and the secondary effect due to deformation of the crystal lattice following the magnetic ordering. It has the same nonzero coefficients as the photoelastic tensor [11,12]. For crystals of trigonal syngony of class D_{3d}, the expanded form of the equation for the corrections to the coefficients of the indicatrix (2), using the abbreviated indices, is[8,12]

$$\frac{\Delta B_m}{l^2} = \begin{pmatrix} \beta_{11} & \beta_{12} & \beta_{13} & \beta_{14} & 0 & 0 \\ \beta_{12} & \beta_{11} & \beta_{13} & -\beta_{14} & 0 & 0 \\ \beta_{31} & \beta_{31} & \beta_{33} & 0 & 0 & 0 \\ \beta_{41} & -\beta_{41} & 0 & \beta_{44} & 0 & 0 \\ 0 & 0 & 0 & 0 & \beta_{44} & 2\beta_{41} \\ 0 & 0 & 0 & 0 & \beta_{14} & \beta_{11}-\beta_{12} \end{pmatrix} \begin{pmatrix} \alpha_1^2 \\ \alpha_2^2 \\ \alpha_3^2 \\ \alpha_2\alpha_3 \\ \alpha_3\alpha_1 \\ \alpha_1\alpha_2 \end{pmatrix}. \tag{3}$$

Here α_i are the direction cosines of the antiferromagnetic vector $l = M_1 = M_2$, and the coordinate system is chosen in the usual manner ($Z \parallel C_3$, $X \parallel U_2$).

In the general case of arbitrary orientation of the vector l, the off-diagonal coefficients of the equations of the optical indicatrix differ from zero and the principal axes of the indicatrix do not coincide with the chosen coordinate axes. The expressions for the angles of the necessary rotations of the initial system of coordinates, which align them with the principal axes of the indicatrix, can be obtained by taking into account the fact that cobalt carbonate is characterized by a large natural linear birefringence. Since $n_0 = n_e \sim 2 \times 10^{-1}$ for this substance, and the appearing magnetic birefringence is usually much less than $\Delta n_M \sim 10^{-4}$, it follows that the deformation of the optical indicatrix should be negligible, and the inclination of its principal axis $n_3 = n_p$ to its initial direction, which is parallel to the C_3 axis, should be small. If the initial coordinate frame is chosen such that $Z' \parallel C_3$ and $Y' \perp l$, then we can write for the successive rotations γ and δ about the X′ axis and the new axis Y″, whereby the principal direction of the indicatrix n_3 is aligned with the axis Z‴, the following expression, which is valid for small γ and δ:

$$\begin{aligned} \operatorname{tg} 2\gamma &= \frac{2[\alpha_3(\alpha_1^2+2\alpha_2^2)\beta_{14} + \alpha_2(3\alpha_1^2-\alpha_2^2)\beta_{41}]}{(\alpha_1^2+\alpha_2^2)^{1/2}(B_0-B_e)}l^2, \\ \operatorname{tg} 2\delta &= \frac{2\alpha_1(3\alpha_2^2-\alpha_1^2)\beta_{41}}{(\alpha_1^2+\alpha_2^2)^{1/2}(B_0-B_e)}l^2. \end{aligned} \tag{4}$$

The directions of the indicatrix n_1 and n_2 are aligned with the corresponding coordinate axes after the obtained coordinate system is rotated through an angle ζ about the direction n_3 (close to C_3):

$$\operatorname{tg} 2\zeta = \frac{2\alpha_1\alpha_3(3\alpha_2^2-\alpha_1^2)\beta_{14}}{2\alpha_2\alpha_3(\alpha_2^2-3\alpha_1^2)\beta_{14} - (\alpha_1^2+\alpha_2^2)^2(\beta_{11}-\beta_{12})}l^2. \tag{5}$$

Here B_0 and B_e are the coefficients of the indicatrix of the paramagnetic crystal. It is seen from the last equation that the antiferromagnetic vector l may not lie in the principal plane of the indicatrix (ζ can be different from zero). In the general case, the value of the angle ζ is determined by the ratio $\beta_{14}/(\beta_{11}-\beta_{12})$ and depends on the direction cosines of l. On the other hand, if l lies in the basal plane or in the symmetry plane, then the angle ζ vanishes, and one of the principal planes of the indicatrix passes through the antiferromagnetic vector.

Assuming that the nonzero components of the tensor β_{ik} are comparable in magnitude, we can estimate the angles γ and δ. In order of magnitude, they are equal to the ratio of the magnetic birefringence to the natural one, $\Delta n_M/(n_0-n_e) \sim 10^{-3}$–$10^{-4}$, which is smaller by almost two orders of magnitude than the angle between the optical axes $[\Delta n_M/(n_0-n_e)]^{1/2}$[9].

Confining ourselves in the determination of the principal refractive indices to terms of first order of smallness, we can neglect the deviation of the direction of n_3 from the C_3 axis, and assume that n_1 and n_2 lie in the basal plane. In this approximation, the expressions for the principal coefficients of the indicatrix take the form

$$\begin{aligned} B_1^0 &= 1/\varepsilon_1^0 = B_0 + \{{}^1/_2(\beta_{11}+\beta_{12})(\alpha_1^2+\alpha_2^2) + \beta_{13}\alpha_3^2 - [{}^1/_4(\beta_{11}-\beta_{12})^2 \\ &\times(\alpha_1^2+\alpha_2^2)^2 + \beta_{14}^2\alpha_3^2(\alpha_1^2+\alpha_2^2) + \beta_{14}(\beta_{11}-\beta_{12})\alpha_2\alpha_3(3\alpha_1^2-\alpha_2^2)]^{1/2}\}l^2, \\ B_2^0 &= 1/\varepsilon_2^0 = B_0 + \{{}^1/_2(\beta_{11}+\beta_{12})(\alpha_1^2+\alpha_2^2) + \beta_{13}\alpha_3^2 + [{}^1/_4(\beta_{11}-\beta_{12})^2 \\ &\times(\alpha_1^2+\alpha_2^2)^2 + \beta_{14}^2\alpha_3^2(\alpha_1^2+\alpha_2^2) + \beta_{14}(\beta_{11}-\beta_{12})\alpha_2\alpha_3(3\alpha_1^2-\alpha_2^2)]^{1/2}\}l^2, \\ B_3^0 &= 1/\varepsilon_3^0 = B_e + \{\beta_{31}(\alpha_1^2+\alpha_2^2) + \beta_{33}\alpha_3^2\}l^2. \end{aligned} \tag{6}$$

The cumbersome expressions of (6) become much simpler if l lies in the basal plane. The principal refractive indices are equal in this particular case to

$$n_1 = n_0 - {}^1/_2 n_0^3 \beta_{12} l^2, \quad n_2 = n_0 - {}^1/_2 n_0^3 \beta_{11} l^2, \quad n_3 = n_e - {}^1/_2 n_e^3 \beta_{31} l^2, \qquad (7)$$

and for the birefringence in the case of light propagating along the principal directions of the indicatrix we can write

$$\begin{aligned} n_1 - n_2 &= {}^1/_2 n_0^3 (\beta_{11} - \beta_{12}) l^2 \quad \text{for } \mathbf{k} \| n_3 \ (\mathbf{k} \| C_3, \perp \mathbf{l}); \\ n_2 - n_3 &= (n_0 - n_e) - {}^1/_2 n_0^3 (\beta_{11} - n_e^3 \beta_{31} / n_0^3) l^2 \quad \text{for } \mathbf{k} \| n_1 \ (\mathbf{k} \perp C_3, \| \mathbf{l}); \\ n_1 - n_3 &= (n_0 - n_e) - {}^1/_2 n_0^3 (\beta_{12} - n_e^3 \beta_{31} / n_0^3) l^2 \quad \text{for } \mathbf{k} \| n_2 \ (\mathbf{k} \perp C_3, \perp \mathbf{l}). \end{aligned} \qquad (8)$$

For light propagating parallel to the trigonal axis, the birefringence does not depend on the direction of the antiferromagnetic vector if $\mathbf{l} \perp C_3$. On the other hand, if the vector l does not lie in the basal plane, then $n_1 - n_2$ becomes dependent on the orientation of the projection $l_\perp$ in the basal plane. The amplitude of the variation of the change of the birefringence upon rotation of $l_\perp$ about the C_3 axis is determined by the ratio $2\alpha_3\beta_{14}/(\beta_{11} - \beta_{12})$. At small α_3, the birefringence is equal to

$$n_1 - n_2 = \frac{1}{2} n_0^3 (\beta_{11} - \beta_{12}) \left[1 + \frac{2\beta_{14}}{\beta_{11} - \beta_{12}} \alpha_2 \alpha_3 (3\alpha_1^2 - \alpha_2^2) \right] l^2. \qquad (9)$$

Knowing the differences between the principal refractive indices, we can determine the angle 2V between the optical axes. This angle, being proportional to $(n_g - n_m)^{1/2}$, depends linearly on the antiferromagnetic vector. The proportionality coefficient, as follows from (6), remains constant when l is rotated about the C_3 axis, provided that $l_z = 0$. Recognizing that the refractive indices n_1 and n_2 are close to each other, $n_1 \approx n_2 \approx n_0$ and $n_3 \approx n_p \approx n_e$, we can express the angle between the optical axes[9] in the case $\mathbf{l} \perp C_3$ in the form

$$2V = 2 \left(\frac{n_e^2 |n_1 - n_2|}{n_0 (n_0^2 - n_e^2)} \right)^{1/2} = 2 n_0 n_e \left(\frac{|\beta_{11} - \beta_{12}|}{2(n_0^2 - n_e^2)} \right)^{1/2} l. \qquad (10)$$

As follows from (8), at $(\beta_{11} - \beta_{12}) > 0$ we get $n_1 = n_g$ and $n_2 = n_m$, and consequently the plane in which the optical axes lie is parallel to the vector l, and at $(\beta_{11} - \beta_{12}) < 0$ it is perpendicular to l. On the other hand, if $l_z \neq 0$ and l does not lie in the symmetry plane, the angle between the plane of the optical axes and the $(\mathbf{l}C_3)$ plane is equal to the angle ξ (5), accurate to $\pi/2$.

The main features of the described optical behavior of cobalt carbonate in magnetic ordering are clearly revealed in the experiments. Figure 2 shows the variation of the conoscopic figures of a $CoCO_3$ crystal at different temperatures, when the crystal is placed in a magnetic field of approximate intensity 6 kOe. The field is parallel to the twofold symmetry axis and is sufficient for saturation[3,4]. The polarizer and analyzer axes are crossed and make an angle of 45° with the vector H. The distances between the branches of the hyperbolas at such a position of the polarizers are maximal, and the vertices of the hyperbolas correspond to the points of emergence of the optical axes. One can clearly see a transition of the crystal from the optically uniaxial state to the biaxial state following the antiferromagnetic ordering. The optical axes lie in the same plane in which the antiferromagnetic vector lies, and their bisector coincides within the limits of experimental error (±0.2°) with the optical axis of the uniaxial crystal. This means that the principal directions of the indicatrix coincide with the coordinate axes X′, Y′, and Z′, with $n_1 = n_g$, $n_2 = n_m$, $n_3 = n_p$, and consequently $(\beta_{11} - \beta_{12}) > 0$.

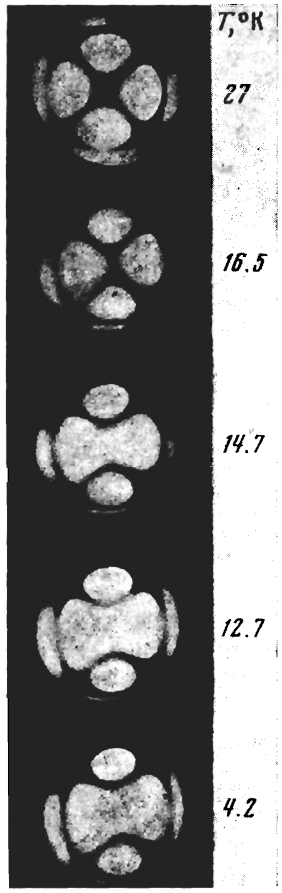

FIG. 2. Conoscopic figures of cobalt carbonate cyrstal as functions of the temperature

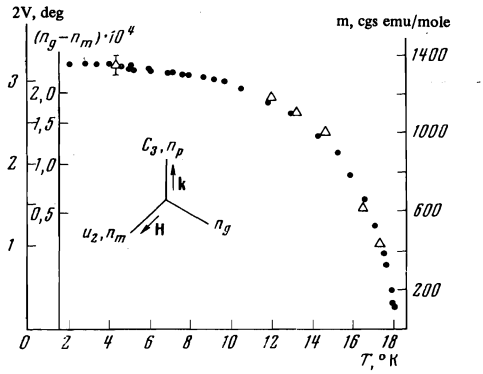

FIG. 3. Temperature dependence of the acute angle 2V between the optical axes and the birefringence $n_g - n_m$ (triangles) and of the spontaneous ferromagnetic moment n_m (circles).

The obtained conoscopic figures were used to calculate the acute angle between the axes. Figure 3 illustrates the dependence of this angle on the temperature. The same figure shows the temperature difference of the ferromagnetic moment m of cobalt carbonate; within several percent, this dependence duplicates the temperature variation of the sublattice magnetization[3]. Within the limits of experimental error, good qualitative agreement is observed in the behavior of both quantities. Knowing the angle between the optical axes and putting $n_0 = 1.855$ and $n_e = 1.600$ for $\lambda = 5890$ Å[6] we can, using (10), calculate the value of the birefringence $n_g - n_m$ that appears following magnetic ordering. This value is indicated on one of the vertical axes of Fig. 3. At 4.2°K, the acute angle between the optical axes of the cobalt carbonate is 3.2 ± 0.2°, and the linear birefringence in the direction of the former optical

axis is $(2.5 \pm 0.15) \times 10^{-4}$. Putting $l = 1.67 \times 10^4$ cgs emu-mole^{-1} [3], we obtain $\beta_{11} - \beta_{12} = 2.8 \times 10^{-13}$ (cgs emu)^2 mole^{-2}.

When the crystal is rotated about the C_3 axis, the angle between the optical axes remains constant, the direction of its bisector remains unchanged, and the plane of the axes also remains perpendicular to H. Consequently, the principal directions of the indicatrix continue to coincide with the coordinate axes X′, Y′, Z′, while the angles γ, δ, and ζ are smaller than the measurement errors. Since the error in the determination of the orientation of the plane of the optical axes is no larger than 5°, it follows from (5) that $(1 - \alpha_3^2)^{1/2}\alpha_3\beta_{14}/(\beta_{11} - \beta_{12}) < 0.1$. The small value of the angle ζ in cobalt carbonate simplifies the use of magnetic birefringence to determine the plane $(1C_3)$ in which the antiferromagnetic vector is located.

4. DOMAIN STRUCTURE

The large value of the magnetic birefringence and the good transparency of cobalt carbonate crystals have made it possible to observe its magnetic domain structure visually during the course of magnetization. In the absence of an external magnetic field, for arbitrary positions of the polarizer and of the analyzer crossed with it, the crystal is practically uniformly darkened, and its conoscopic figure, which is typical of uniaxial crystals, remains unchanged when the sample is cooled to temperatures below T_N. Conoscopic figures characteristic of biaxial crystals are observed only when the sample is placed in a sufficiently strong magnetic field. This fact allows us to state that either the magnetic structure of $CoCO_3$ is helicoidal, or that the sample becomes laminated into flat thin domain layers directed parallel to the basal plane, and the angles between the directions of the magnetic moments in neighboring layers are not equal to 180°. The second assumption seems more probable, since cobalt carbonate is characterized by a large value of the magnetic-anisotropy energy [4,13].

We have attempted to observe the emergence of the presumed planar domains parallel to the basal plane on an oblique surface of a wedge-shaped sample. One surface of the prepared sample was perpendicular to the trigonal axis, and the angle between the second surface and the first was about 18°. The surface of the sample measured 1.5×10 mm. Its thickness varied from 0.2 to 0.7 mm. The attempt was unsuccessful, possibly because of the small thickness of the domain layer and the presence of closing domains. We noted only that individual smeared-out sections of the sample became slightly transparent.

Application of a magnetic field with approximate intensity 10 Oe and with an intensity vector lying in the basal plane leads to a noticeable bleaching of individual sections of the crystal. The boundaries of the light and dark sections are at first blurred, but even a field of 20—30 Oe suffices to make them sharper, and in fields from 50 to 120 Oe one observes domain bands with sharp boundaries. With increasing field intensity, the width of the bands decreases from 200 to 10 μ, their number increases, and in a field of approximately 160 Oe (T = 12°K) they are no longer visible. In a decreasing field, the domain bands appear approximately in the same places, but at different values of the intensity (see Fig. 4). The boundaries of most bands are most frequently parallel to the vertical symmetry planes, although boundaries having different orientations are also encountered.

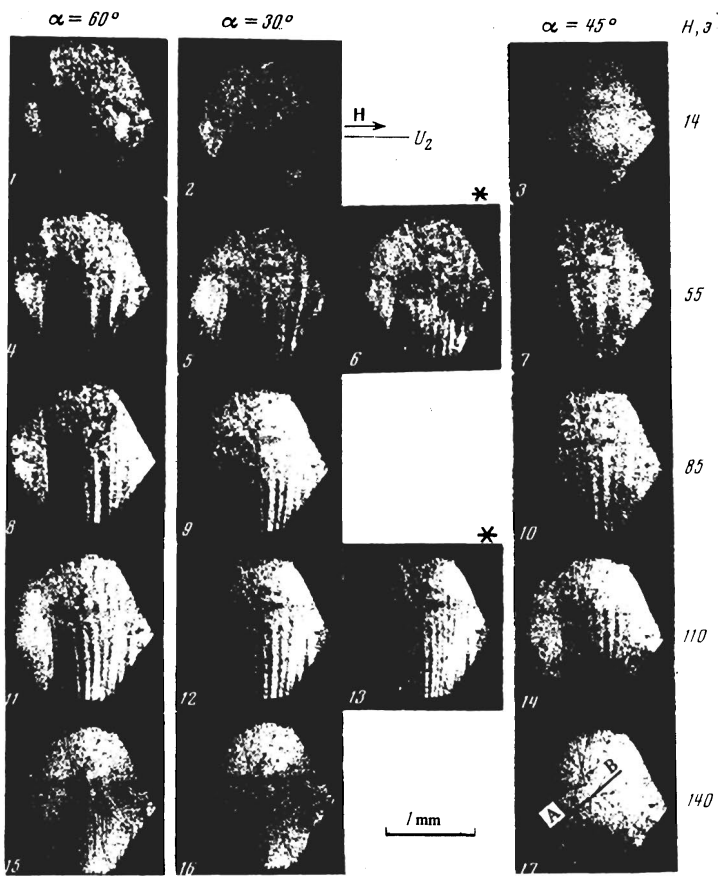

FIG. 4. Domain structure of cobalt carbonate in magnetic field. Magnetic field $\mathbf{H} \parallel U_2$, sample temperature 12°K, azimuth α of the polarizer measured from the direction of the U_2 axis. The photographs marked by asterisks were obtained with decreasing field. The line AB on the last figure is parallel to the lines of the equal-thickness wedge; the sample thickness increases from 0.2 to 0.7 towards the lower right corner of the photographs.

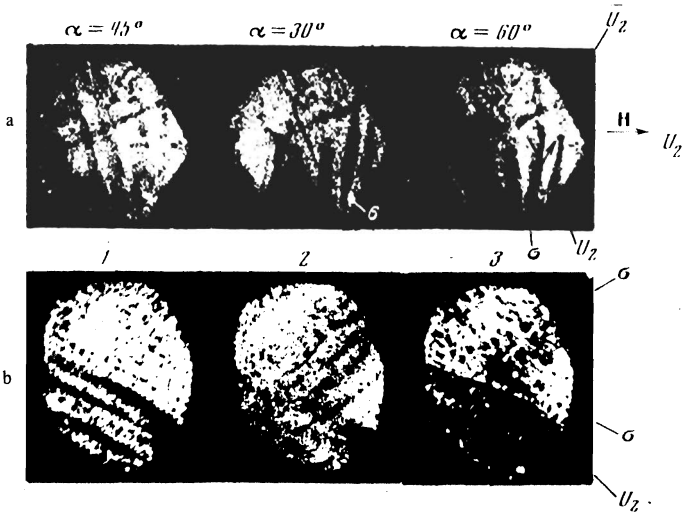

FIG. 5. Orientation of the domain broundaries: a—manifestations of the different domains following variation of the polarizer azimuth α; b—appearance of domain systems upon rotation of the magnetic field in the basal plane of the crystal.

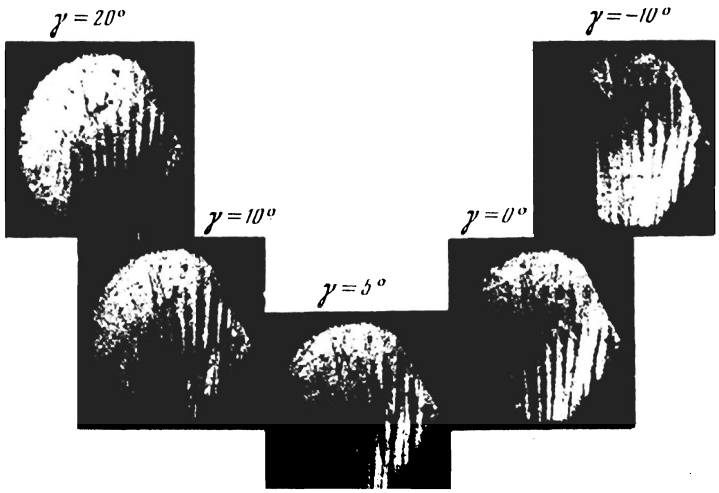

FIG. 6. Different views of one and the same magnetic domain structure of $CoCo_3$ (H = 120 Oe, T = 12°K, $H \parallel U_2$) as a function of the ellipticity (tan γ) of the light incident on the sample. The analyzer is oriented at an angle 90° to the major axis of the polarization ellipse of the incident light, the azimuth of which is contant and equal to 75°.

Simultaneous rotation of the crossed polarizer and analyzer reveals the simultaneous existence in the crystal of different systems of bands, which are projected on one and the same section of the sample surface (Figs. 4 and 5a). At definite azimuths of the polarizers, they can be observed simultaneously. Domain bands with approximately 60° angles between then can be seen in photographs 5 and 6 of Fig. 4 and on photograph 2 of Fig. 5a (lower right corner). On photographs 1 and 4 of Fig. 4 one can see domain bands that intersect at angles of 20—30°. If the magnetic-field vector is rotated relative to the direction of the crystallographic symmetry axis, then the systems of intersecting bands can be seen more clearly. Figure 5 shows photographs obtained at the same azimuth of the polarizer in a field having the identical intensity, but different directions in the basal plane of the crystal. When the field is parallel to the twofold axis (photograph 1), one can see one system of bands, and when it is inclined away from the axis (photographs 2 and 3), new systems of bands that intersect the preceding ones can be observed. Their boundaries lie either in the symmetry plane or in the plane of the two- and threefold crystallographic axes. The bending of the boundaries, which is noticeable on all the photographs, is apparently connected with the fact that the sample is wedge-shaped and with the internal stresses in the crystal. The intensity of the light passing through the intersection of the bands differs from the intensity of the light passing through individual bands, and their ratio depends on the azimuth of the polarizer. The boundaries of simultaneously existing bands of different systems are displaced independently in a magnetic field. All these facts indicate that the observed domain systems are situated at different depths in the crystal. This is seen particularly convincingly when the bands move relative to one another in a varying magnetic field.

When observing the domain structure at a fixed azimuth of the polarizer, one might think that in a field of approximately 100 Oe and more the domain structure becomes simpler (there remain bands perpendicular to the field, see photographs 12—14 of Fig. 4). However, this simplicity is illusory, since the extinction angle does not remain constant within the limits of the band (photos 11—14 of Fig. 4). A compensator of the Senarmont type can be used to observe the variation, over the surface of the crystal, of the ellipticity and the azimuth of the principal axis of the polarization ellipse of the light emerging from the sample. The polarizer and analyzer were initially crossed, and the azimuth of a quarter-wavelength phase plate placed ahead of the sample coincided with the azimuth of the polarizer. Rotation of the polarizer through an angle γ with the quarter-wave plate and analyzer both stationary leads to darkening of those sections of the sample which convert the elliptically polarized light with the azimuth of the quarter-wave plate and ellipticity tan γ into linearly

polarized light with the same azimuth. The photographs shown in Fig. 6 were obtained at different azimuths of the polarizer and fixed azimuths of the $\lambda/4$ plate and of the analyzer. The obtained distribution of the light polarization over the surface of the sample is attributed to the presence of domain layers parallel to the basal plane. The transverse domain walls in neighboring layers, as follows from Fig. 6, should be slightly out of parallel to one another.

A similar domain structure, containing both transverse ($S_\perp$) and longitudinal ($S_\parallel$) domain boundaries, was observed with the aid of the Faraday effect[14] and by the method of polarized neutrons[15] in hematite, where the transverse boundaries were observed in the absence of an external field. The simultaneous existence of $S_\parallel$ and $S_\perp$ boundaries is due to their energy proximity[16]. The absence of transverse domain boundaries in cobalt carbonate and their appearance when an external magnetic field is turned on points to the presence of a dependence of the energy $S_\parallel$ and $S_\perp$ boundaries on the intensity of the magnetic field. The reason for the different behavior of the boundaries in a magnetic field may be the difference between the magnetic moments of the $S_\parallel$ and $S_\perp$ domain walls.

The multilayer character of the domain structure of $CoCO_3$ makes it difficult to determine the angle of rotation of the magnetic moment on going through the domain boundary. However, even the fact that the domains are observable when the polarizers are crossed indicates that the walls are not of the 180° type. Moreover, it was noted that on one section of the crystal the extinction angles of the domain bands, the boundaries of which lie in the symmetry plane, are close to 30 and 60°. Measurement of the ellipticity of the light emerging from these domains has shown that it is close to the ellipticity of the light passing through the same section of the sample saturated to magnetization. It was thus established that the transverse boundaries cut through the entire sample in this place. The reason for this may be the internal stresses in the crystal. By determining the directions of the axes n_g and n_m with the aid of a half-wave plate, it was found that the angle between the antiferromagnetic vectors, and consequently between the ferromagnetic moments of the neighboring domains, is 120°, and that the directions of the magnetic moments coincide with the directions of the twofold symmetry axes (photo 3, Fig. 5a).

5. CONCLUSIONS

From the obtained experimental results we can draw the following conclusions.

1. The linear birefringence that appears in the case of magnetic ordering for light propagating along the trigonal axis of cobalt carbonate, is of the order of 2.5×10^{-4} at 4.2°K and makes possible visual observations of the magnetic domain structure. One of the principal axes of the optical indicatrix n_g is parallel to the plane passing through the antiferromagnetic vector and the trigonal axis, and the other, n_m, coincides with the direction of the ferromagnetism vector.

2. In the absence of an external magnetic field, the magnetic structure of cobalt carbonate is either homogeneous and helicoidal, or else the crystal breaks up into helicoidal domains parallel to the basal plane, and in the latter case the domain walls are not of the 180° type.

3. The manner in which the domain bands appear in a magnetic field, namely the appearance first of smeared-out regions and their subsequent formation into broad bands, followed by narrowing and increase in their number, leads to the conclusion that the external magnetic field induces the appearance of $S_\perp$ walls. The predominant transverse walls are of the 120° type parallel to the vertical symmetry planes. The magnetic domain structure of cobalt carbonate in a magnetic field can be represented in the form of plane layers parallel to the basal plane which, in turn, are broken up by transverse walls into parallel bands. The transverse walls tend to lie perpendicular to the magnetic-field vector and parallel to the symmetry planes.

The authors take the opportunity to thank A. S. Borovik-Romanov and N. M. Kreĭnes for useful discussions of the results of the work, and N. Y. Ikornikov and V. Egorov for supplying the single-crystals of synthetic cobalt carbonate.

[1] M. M. Farztdinov, Usp. Fiz. Nauk 84, 611 (1964) [Sov. Phys.-Uspekhi 7, 855 (1965)].
[2] R. V. Pisarev, I. G. Siniĭ, and G. A. Smolenskiĭ, ZhETF Pis. Red. 9, 112, 294 (1969) [JETP Lett. 9, 64, 172 (1969)].
[3] A. S. Borovik-Romanov and V. I. Ozhogin, Zh. Eksp. Teor. Fiz. 39, 28 (1960) [Sov. Phys.-JETP 12, 18 (1961)].
[4] Ya. J. Katzer, ibid. 43, 2042 (1962) [16, 1443 (1963)].
[5] R. A. Alikhanov, ibid. 39, 1481 (1960) [12, 1028 (1961)].
[6] A. N. Winchell and H. Winchell, Optical Properties of Artificial Minerals, Acad. Press, 1964.
[7] A. I. Belyaev, V. V. Eremenko, I. I. Mikhaĭlov, and S. V. Petrov, Zh. Eksp. Teor. Fiz. 49, 47 (1965) [Sov. Phys.-JETP 22, 33 (1966)].
[8] J. Nye, Physical Properties of Crystals, Oxford, 1957.
[9] L. D. Landau and E. M. Lifshitz, Elektrodinamika sploshnykh sred (Electrodynamics of Continuous Media), Gostekhizdat, 1959 [Pergamon, 1959].
[10] R. V. Pisarev, Zh. Eksp. Teor. Fiz. 58, 1421 (1970) [Sov. Phys.-JETP 31, 761 (1970)].
[11] S. Bhagavantan, Mat. Res. Bull., 4, 477 (1969).
[12] R. R. Birss, Rept. Progr. Phys., 26, 307 (1963).
[13] J. Kaczer, Czech. J. of Phys., 12, 354 (1962).
[14] H. J. Williams, R. C. Sherwood, and J. P. Remeika, J. Appl. Phys., 29, 1772 (1958).
[15] R. Nathans, Phys. Rev., 136, 6A, 1641 (1964).
[16] M. M. Farztdinov, Izv. Akad. Nauk SSSR 28, 590 (1964).

Translated by J. G. Adashko
148